EM Implosion Memos

Memo 50

July, 2010

Experimental results for the focal waveform and beam width in air with a 100 ps filter

Prashanth Kumar, Carl E. Baum, Serhat Altunc, Christos G. Christodoulou and Edl Schamiloglu
University of New Mexico
Department of Electrical and Computer Engineering
Albuquerque, NM 87131

Abstract

This paper presents experimental results for the focal waveform and beam width in air with a 100 ps filter. The filter is characterized to ensure that it performs within the desired specifications. The focal impulse waveform and the beam width are compared to the rescaled results in [1]. The experimental results are found to agree well with analytical calculations and numerical simulations.

1 Introduction

The experimental results in [1] were obtained using a 45 ps pulser. To remain consistent with our analytical calculations and numerical simulations, which assume an input with a 100 ps rise, the experimental focal impulse waveform in air was rescaled so that its FWHM was 100 ps. Consequently, the beam width in air had to be rescaled in a similar manner.

The rescaling technique assumes that the experimental, Gaussian-shaped, impulsive part of the waveform can be analytically approximated by an ideal rectangular pulse, as shown in the sketch in Fig. 1.1 (the areas under all the curves are the same). The width of the rectangular pulse is identical to the FWHM of the impulse. Due to these inherent approximations, the rescaling method is accurate only to first order as it does not take into account all components of the response in the frequency spectrum.

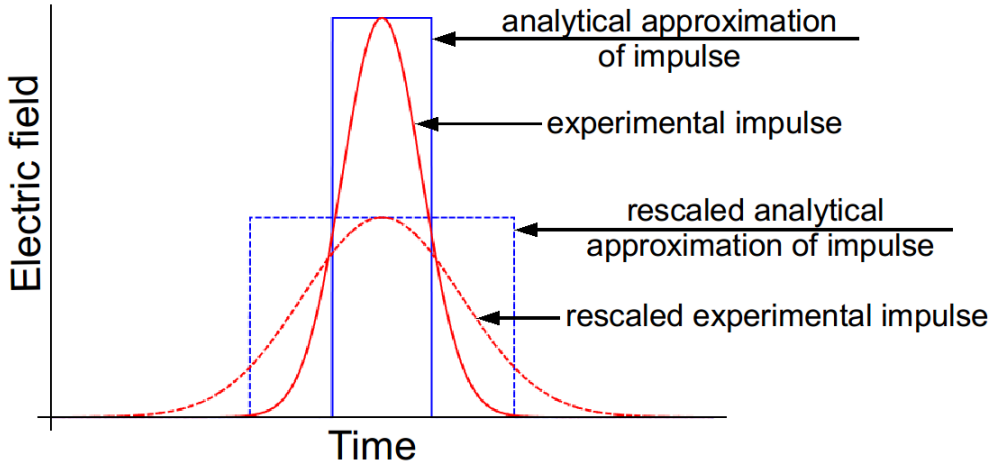

Figure 1.1: Method used to rescale the experimental focal impulse waveform in air [1].

There are two, more accurate methods to obtain results with a 100 ps input,

- Software filter: The focal impulse waveforms obtained with a 45 ps input can be numerically convolved with the desired, 100 ps, input waveform.
- Hardware filter: The simpler, and perhaps more expensive, method is to use a hardware filter. Such low-pass filters are made to desired specifications by Picosecond Pulse Labs. This is the method used in our experiments to measure the focal impulse waveform and beam width, in air and inside the lens, with a 100 ps input.

2 Characterization of the 100 ps filter

The filter was custom designed by Picosecond Pulse Labs to stretch the 45 ps input pulse obtained from the setup in [1] to a pulse with a 100 ps rise time while maintaining the same peak amplitude ($\pm$ few mV). The S_{11} and S_{21} measurements from the data sheet[1] are reproduced in Fig. 2.1. One notes that the return loss is less than -15 dB upto 5 GHz and the insertion loss falls from 0 dB

[1] `http://www.picosecond.com/product/category.asp?pd_id=4`

to −18 dB from 0 to 5 GHz. The low return and insertion losses of the filter are a pre-requisite for our experiments.

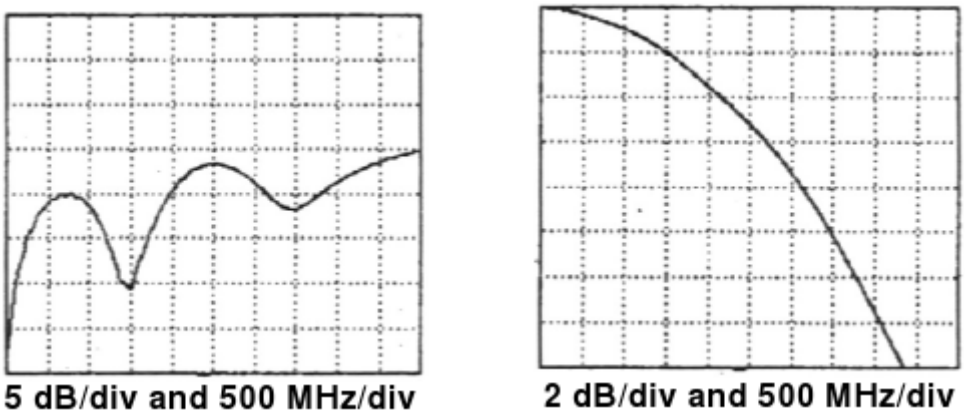

(a) S_{11} Return loss (b) S_{21} Insertion loss

Figure 2.1: Return loss and insertion loss measurments from 5915-X specsheet from Picosecond Pulse Labs.

Fig. 2.2 shows the setup to measure the output of the 45 ps pulse generator with the filter. To

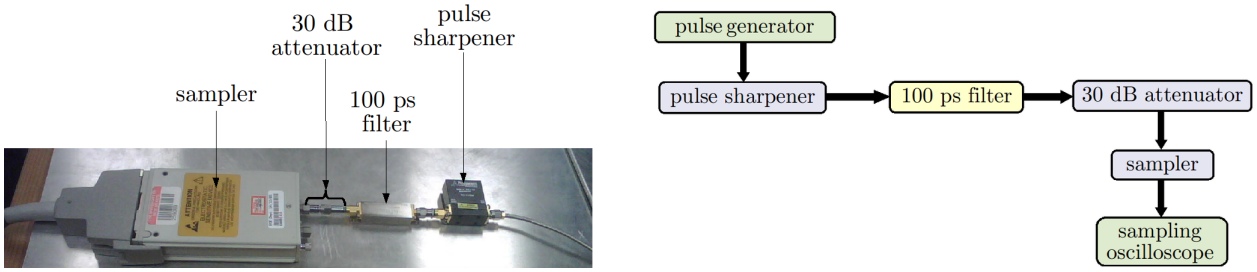

(a) Attenuator, filter and sharpener (b) Block diagram: Attenuator, filter and sharpener

Figure 2.2: Setup: Attenuator, filter and sharpener.

characterize the performance of the filter the shape, peak amplitude and rise time of the output waveform are examined. The filter is considered to operate within desired specifications if the output waveform,

1. Has the same shape as the waveform obtained without the filter.
2. Rises from 0 V to a peak amplitude of 10 V.
3. Has a maximum rate of rise given by a 100 ps pulse.

Fig. 2.3 compares the waveforms from the pulser with and without the filter. The waveform with the filter has the same shape (compared to that without the filter) and a peak amplitude of approximately 10 V. Reflections from the sampler are an experimental concern as they can signficantly affect the output waveform [Fig. 2.2(b)]. Fig. 2.3 indicates that these reflections are negligible.

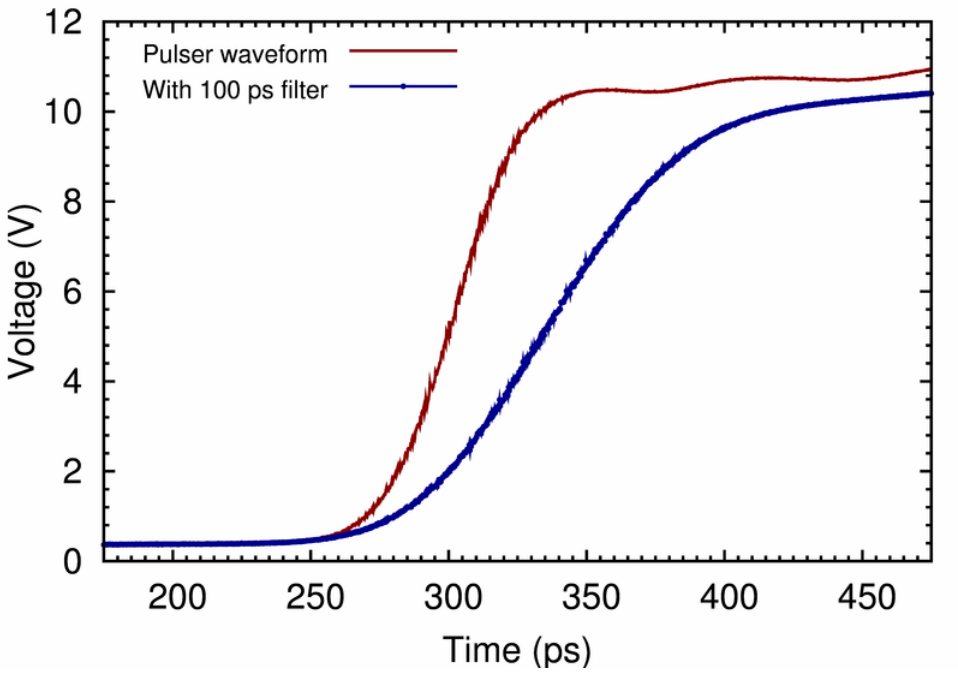

Figure 2.3: Comparison of pulser waveforms with and without filter.

Maximum rate of rise, $t_{\mathbf{mr}}$

For a step, like $f(t)$, the maximum rate of rise, t_{mr} , is defined as [2]

$$t_{\mathrm{mr}} = \frac{f_{\max}}{\left[\frac{df}{dt}\right]_{\max}}. \tag{2.1}$$

Since it is easier to determine the derivative, $(df/dt)_{\max}$, analytically, a generalized logistic function of the form,

$$V = \frac{a}{1 + be^{-ct}} + d, \tag{2.2}$$

is fit to the experimental data, as shown in Fig. 2.4. Note that since we have a voltage waveform the t_{mr} is defined as,

$$t_{\mathrm{mr}} = \frac{V_{\max}}{\left[\frac{dV}{dt}\right]_{\max}}. \tag{2.3}$$

The coefficients for the curve fit in Fig. 2.4 are $a = 10.509$, $b = 376824$, $c = 0.00944$, and $d = 0.22718$, using which the t_{mr} is determined as 100.83 ps.

Thus, the shape, peak amplitude and t_{mr} of the pulser waveform with the filter are as expected and the filter operates to our desired specifications.

It was also found that including additional cables in the setup in Fig. 2.2 (for e.g., between the filter and the sampler) increases the t_{mr} . Therefore, the use of cables is minimized.

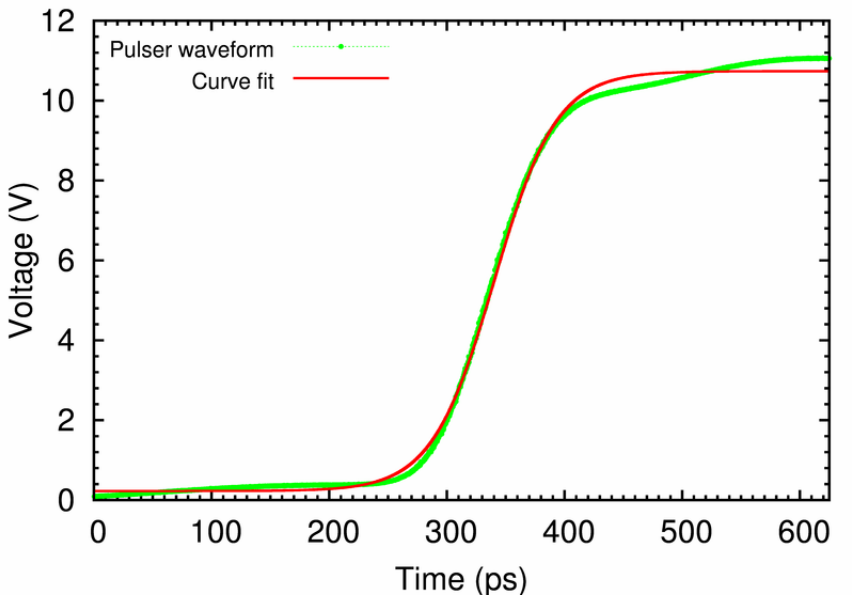

Figure 2.4: Pulser waveform with 100 ps filter.

3 Calibration of the D-dot probe in air

The handmade D-dot probe [1] is calibrated in air using the prepulse. The electric field is obtained from the voltage response of the probe as follows.

The current, I, measured by the D-dot probe is related to its equivalent area, A_{eq}, and voltage, V, as

$$I = \frac{V}{Z_c} = A_{eq}\frac{dD}{dt}, \tag{3.1}$$

where $Z_c = 50\ \Omega$ is the characteristic impedance of the cable connecting the probe to the sampling oscilloscope. Given dD/dt, the electric field can be calculated as

$$E = \frac{1}{\epsilon Z_c A_{eq}} \int_{-\infty}^{t} V(t')dt', \tag{3.2}$$

where $\epsilon = \epsilon_0\epsilon_r$ is the relative permittivity of the medium surrounding the probe. For the experiment under consideration, $\epsilon_r = 1$, as the probe is in air. Since the experiments use a four feed-arm PSIRA over a ground plane, the feed arm impedance is 100 Ω. The voltage transmitted to the feed arms from the pulse generator is,

$$V = TV_0, \quad T = \text{transmission coefficient} = \frac{2Z_l}{Z_l + Z_c} = \frac{2(100)}{100 + 50} = 1.33. \tag{3.3}$$

The electric field measured by the D-dot probe is normalized to a 1 V input as

$$E_N = \frac{1}{20T\epsilon Z_c A_{eq}} \int_{-\infty}^{t} V(t')dt'. \tag{3.4}$$

The theoretical value of the prepulse in air is $E_{pa} = -0.7$ V. The prepulse measured by the probe, normalized to a 1 V input is,

$$E_{pa}^{\text{measured}} = \frac{1}{20T\epsilon_0 Z_c A_{eq}} \int_{-\infty}^{t} V(t')dt', \tag{3.5}$$

where $T = 1.33$, $Z_c = 50\ \Omega$ and $A_{eq} = 10^{-4}\text{m}^2$. We require that the measured prepulse be E_{pa}. For this we multiply the measured electric field by the calibration factor, $\mathcal{C}_a$,

$$\mathcal{C}_a = \frac{E_{pa}}{E_{pa}^{\text{measured}}}. \tag{3.6}$$

4 Experimental Setup

The setup, to measure the focal impulse waveform and the beam width in air, is identical to that in [1], without the focusing lens and the target medium, except that a 100 ps filter is placed between the D-dot probe and the sampler, as shown in the block diagram in Fig 4.1. The filter is connected to the end of the SMA cable from the D-dot probe. No cables are used to connect the filter to the sampler.

Of course, in theory, the filter can be placed anywhere in the setup since the system is linear. However, in our experimental setup, placing the filter at the first focal point was difficult. The setup in Fig 4.1 was found to minimally perturb the measurements and results.

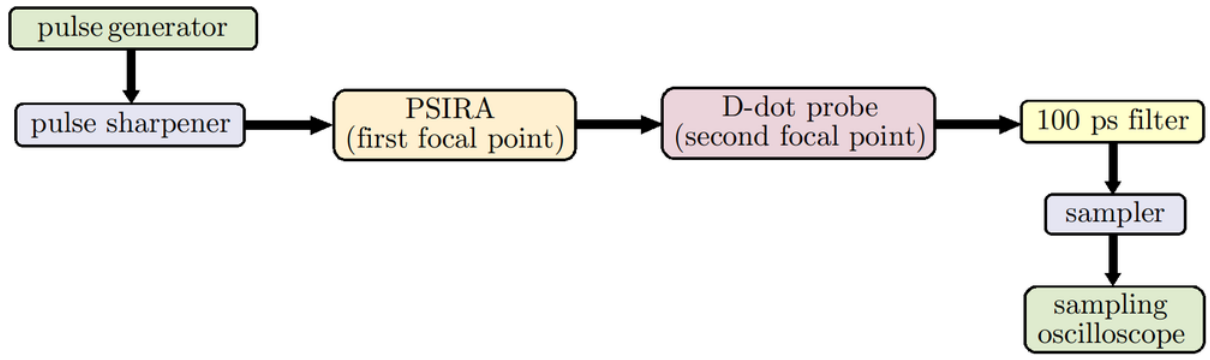

Figure 4.1: Block diagram of the experimental setup. The filter is placed between the D-dot probe and sampler.

5 Results

5.1 Focal impulse waveform

The raw and integrated D-dot probe signals, at the second focal point, in air, with the 100 ps filter are shown in Fig. 5.1. The corresponding normalized electric field focal impulse waveform is shown in Fig. 5.2.

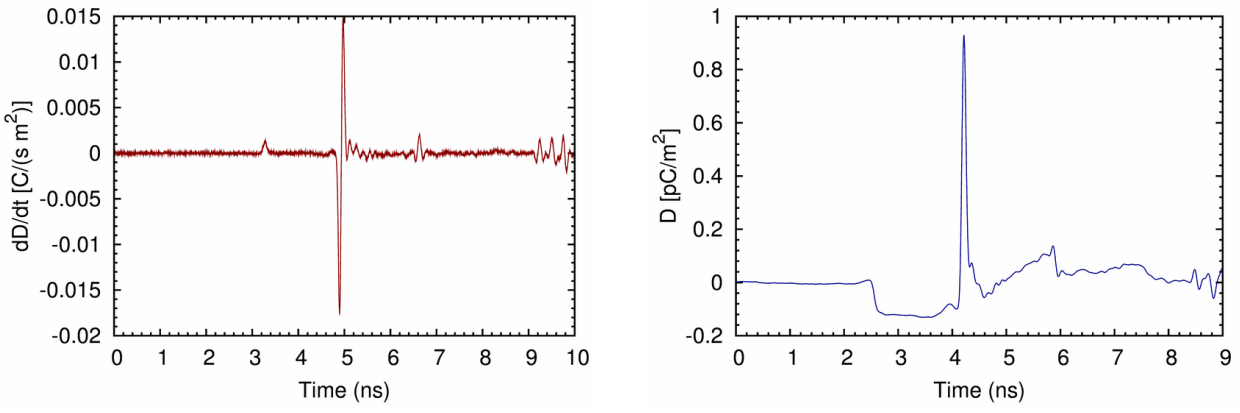

(a) Raw D-dot probe signal

(b) Intergrated D-dot probe signal

Figure 5.1: "Raw" and integrated D-dot probe signal.

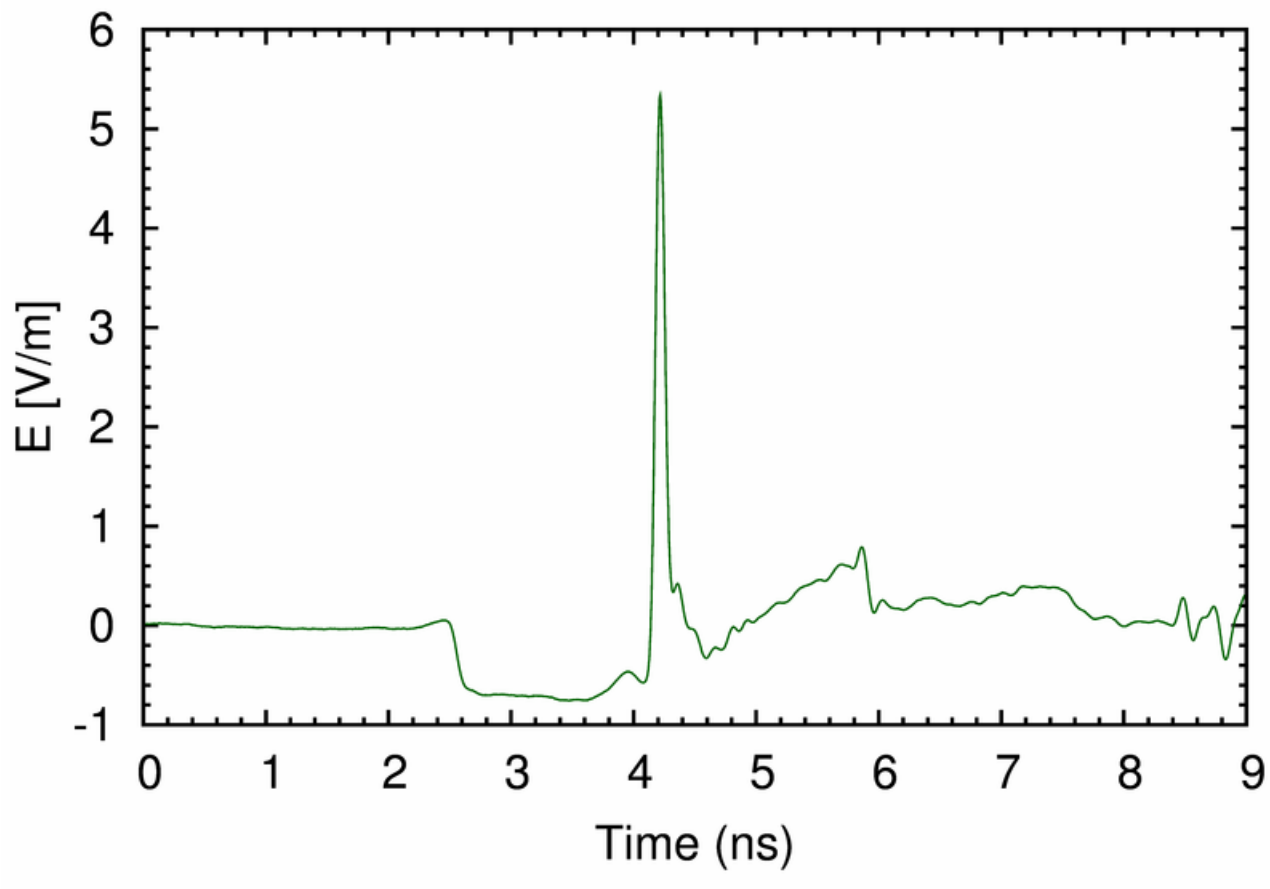

Figure 5.2: Electric field focal waveform in air with 100 ps filter.

The distance between the geometrical focal points is 75 cm. The tip of the D-dot probe is at $z = +3$ mm from the second focal point, i.e., the D-dot probe is at a distance of 75.3 cm ($75 + z$) from the (geometrical) first focal point. The time taken for the wave to travel from the first focal point to the probe tip is

$$\frac{75.3 \text{ cm}}{3 \times 10^8 \text{ cm/s}} \approx 2.51 \text{ ns} \tag{5.1}$$

In the experiments, the time at which the prepulse is registered by the oscilloscope is not what one would expect from (5.1) as there is no fixed time of reference. A more accurate method of making the measurements is to place a second D-dot probe at the first focal point. The second D-dot probe can be used to determine the relative time of arrival of the electric fields measured by the probe at the second focal point. One should also note that the cables connecting the handmade D-dot probe to the oscilloscope introduce a time lag in the data measured by the probe. This time lag is not accurately known and would also introduce time shifts in the fields measured by the probe. The waveforms in Fig. 5.1(b) and Fig. 5.2 are shifted so that the prepulse starts at 2.51 ns. The "zoomed-in" view of the electric field impulse is shown in Fig. 5.3.

The peak electric field amplitude is $E_{\max} = 5.34$ V/m. The pre-pulse, impulse and post-pulse are considered as three separate events, i.e., the impulse can be considered to be super-imposed on the pre-pulse. Therefore, the amplitude of the impulse, E^{I}, is calculated with respect to the average of the start and end of the impulse event; $E_s^i = -0.6$ V/m and $E_e^i = 0.4$ V/m, as shown in Fig. 5.3, i.e.,

$$\Upsilon = \left| \frac{E_s^i + E_e^i}{2} \right| = 0.1 \text{ V/m}, \tag{5.2}$$

and

$$E^{\mathrm{I}} = E_{\max} + \Upsilon = 5.44 \text{ V/m}. \tag{5.3}$$

The FWHM, as determined numerically from the experiment data, is 85 ps as shown in Fig. 5.3. One would expect the FWHM to be identical to the t_{mr} of the input pulse ($t_{\mathrm{mr}} = 100$ ps). The reason for this discrepancy is that the higher frequencies in the input pulse are better focused than the lower frequencies, i.e., the focusing action itself filters out lower frequency content in the focused waveform. Similar results observed in simulations corroborate the above hypothesis.

The electric field focal waveform with the filter is compared to that without the filter ($t_{\mathrm{mr}} = 45$ ps) and the rescaled waveforms from [1], in Fig. 5.4. The plots have been time shifted for clarity. The peak focal impulse amplitude, $E_{\max}$, without the filter is 11.33 V/m and that of the rescaled waveform is 5.67 V/m [$11.33 \cdot (45 \text{ ps}/100 \text{ ps})$]. One thus notes that the peak impulse amplitude of the rescaled waveform and the waveform with the filter are almost the same.

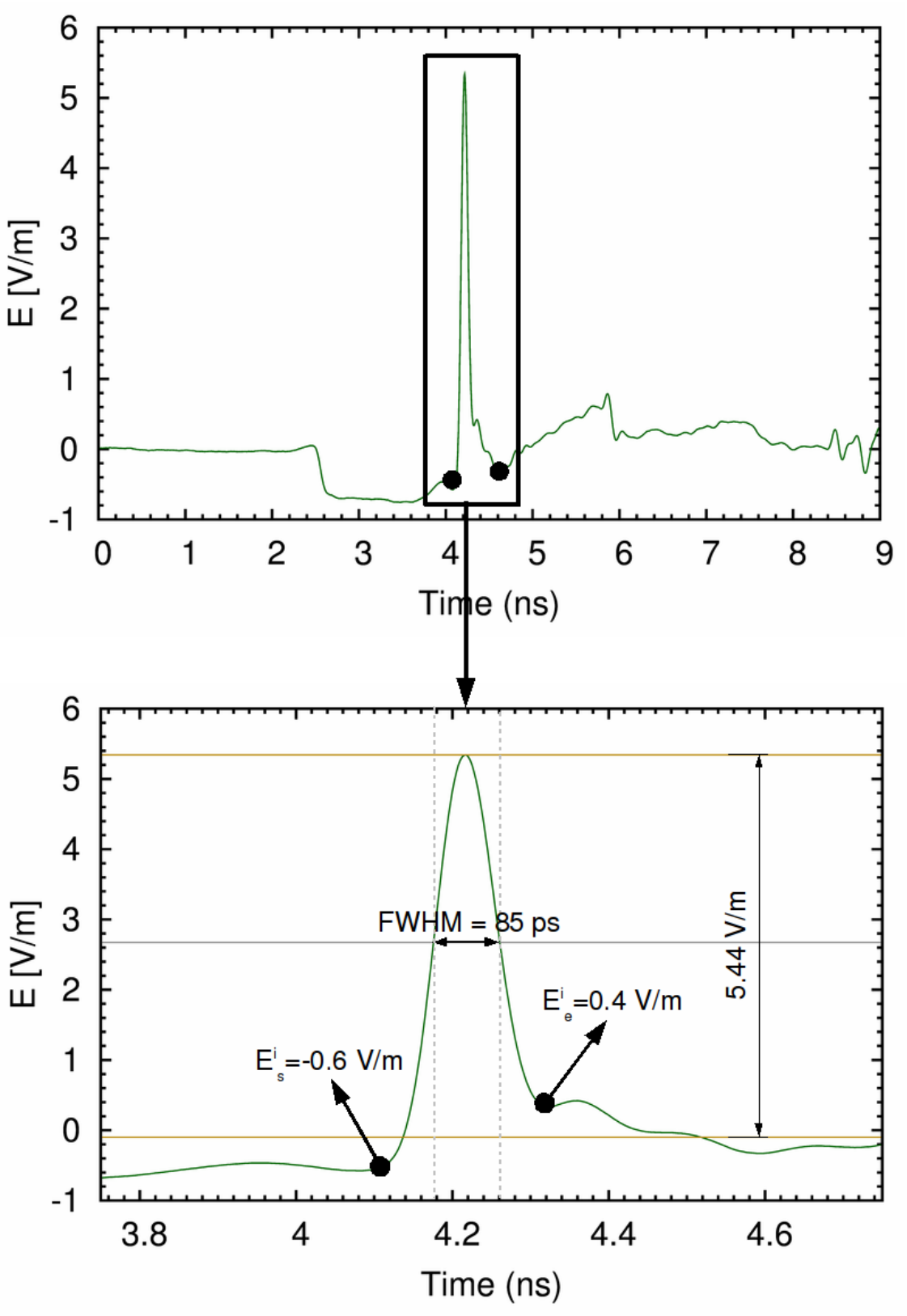

Figure 5.3: "Zoomed-in" view of electric field impulse at second focal point in air with 100 ps filter.

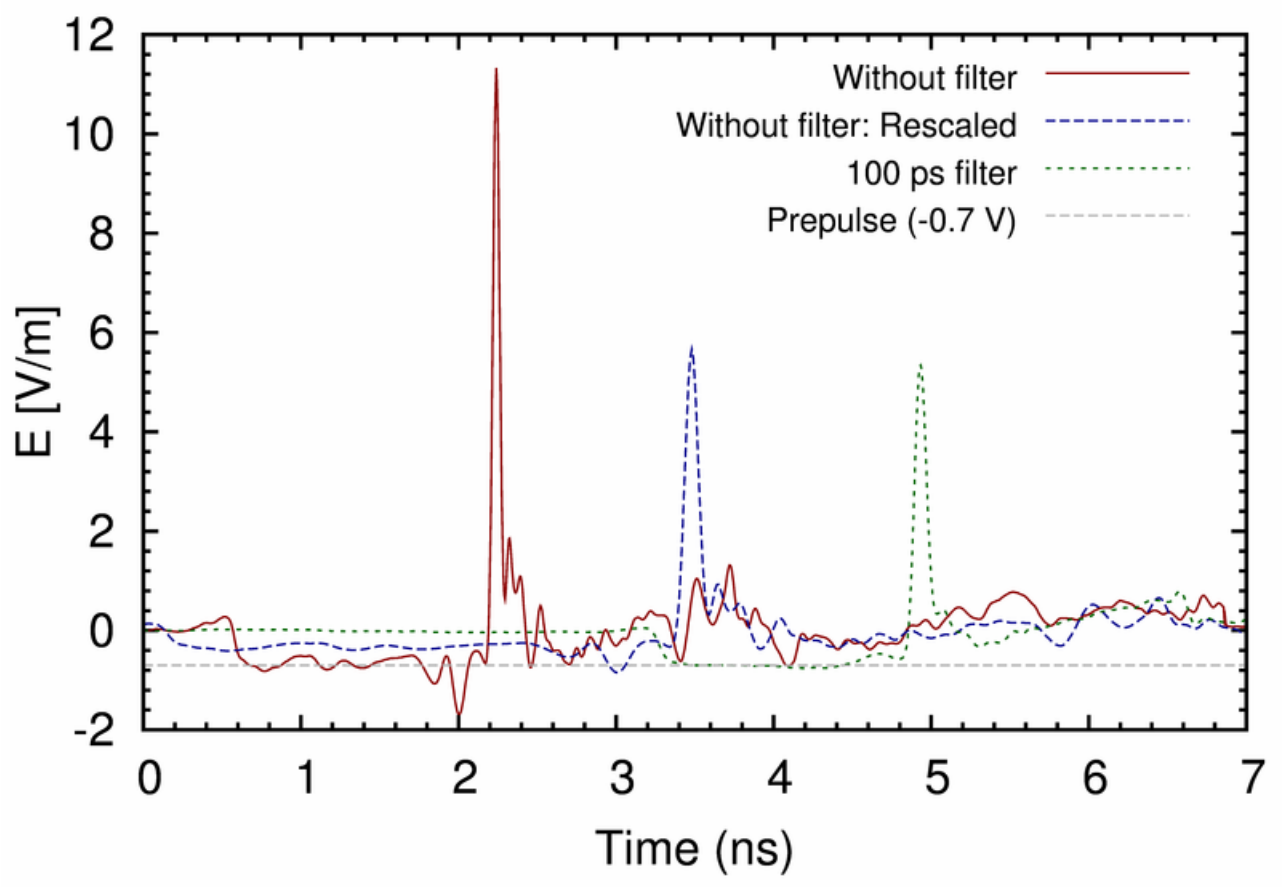

Figure 5.4: Comparison of the electric field focal impulse waveforms with and without the 100 ps filter. The analytical prepulse (-0.7 V) is plotted for reference.

6 Beam width (Spot size)

The beam width (spot diameter), in air, is shown in Fig. 6.1. The error in measurement is approximately ±5%. The data points do not lie along a smooth curve and this makes it difficult to determine the spot size. Therefore, a Gaussian curve of the form

$$f(x) = ae^{-b(x+c)^2+d} + e, \tag{6.1}$$

was fit to the data, where x is the distance along the x-axis from the focal point. The fit parameters are $a = 0.839$, $b = 0.106$, $c = 0.213$, $d = 1.525$, $e = 1.439$. The spot diameter, as determined from the fit, is 4.397 cm.

The beam width from experiments is compared to that obtained from numerical simulations in Fig. 6.2. One observes that the geometrical focal point in the experiments is shifted by approximately $x = +0.25$ cm. This is most likely due to the misalignment of the reflector. The spot diameter in the numerical simulations was 3.610 cm [1], i.e., the experimental beam width is 22% greater than that in the simulation. The beam width from the rescaled waveform is 4.59 cm [1] which is almost identical to that measured with the filter.

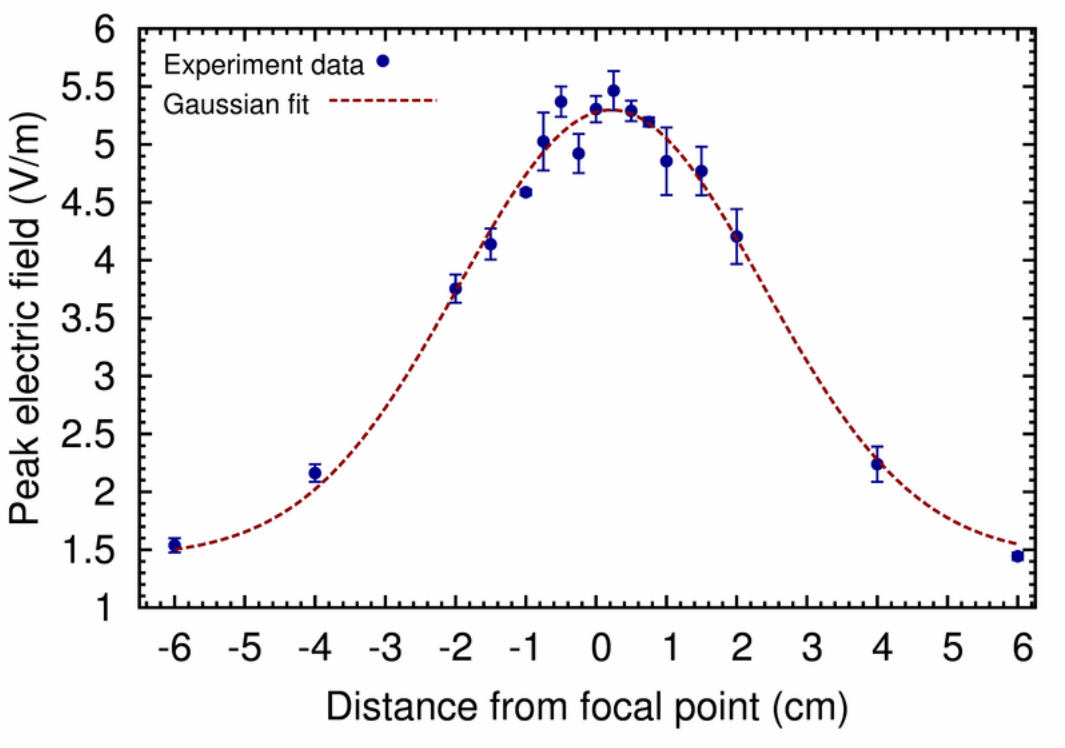

Figure 6.1: Beam width in air and Gaussian curve fit.

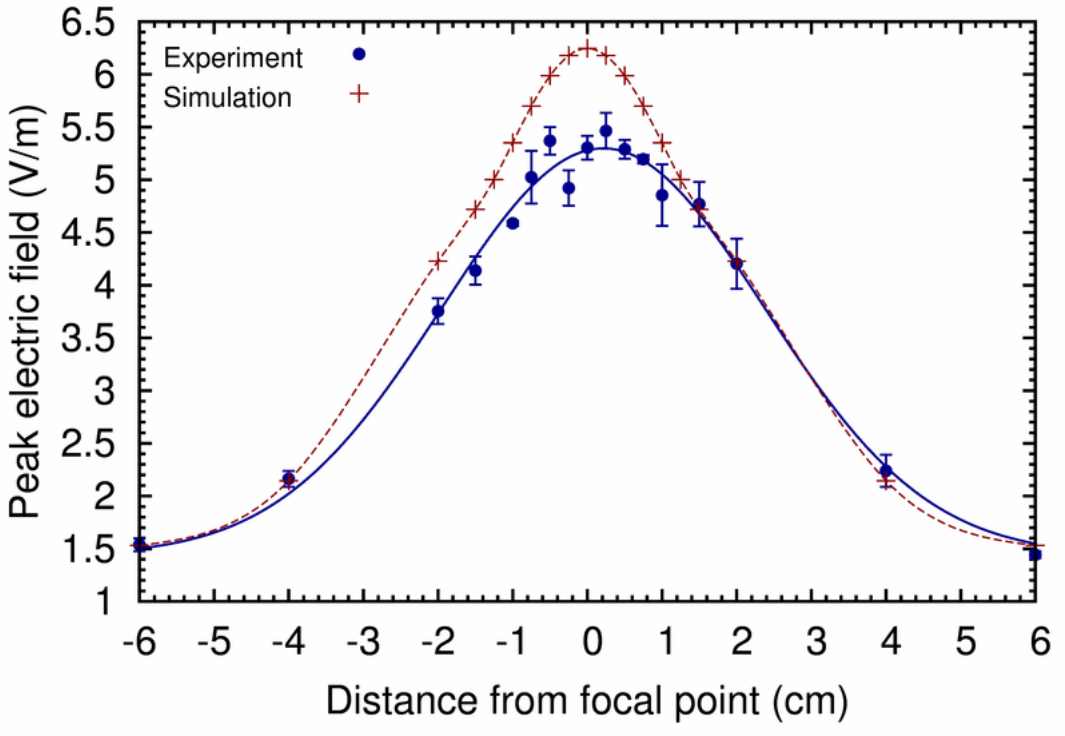

Figure 6.2: Comparison of spot size obtained from experiment and numerical simulation.

7 Conclusions

The 100 ps filter works as expected, as confirmed by examining the output waveform from the pulser with the filter. The focal impulse waveform, in air, with the filter is almost identical to the rescaled waveform in [1]. The amplitude of the impulse is $E^{\mathrm{I}} = 5.44$ V/m. The FWHM is 85 ps, not 100 ps, as the lower frequencies are not focused as effectively as the higher frequencies in the input pulse. The beam width is also almost identical to the rescaled beam width in [1]. It is approximately 22% larger than the spot size obtained from numerical simulations.

References

[1] P. Kumar, S. Altunc, C. E. Baum, C. G. Christodoulou, E. Schamiloglu, and C. J. Buchenauer, "Radially Inhomogeneous Spherical Dielectric Lens for Matching 100 ps Pulses into Biological Targets," *Accepted for publication, IEEE Transactions Plasma Science, Special Issue - Nonthermal Medical/Biological Applications Using Ionized Gases and Electromagnetic Fields*, 2010.

[2] S. Altunc, *Focal Waveform of a Prolate-Spheroidal Impulse Radiating Antenna (IRA).* PhD thesis, University of New Mexico, December 2007.